

This is the peer reviewed version of the following article:

Photovoltaic Cell Modeling for Solar Energy Powered Sensor Networks / Dondi, Denis; D., Brunelli; L., Benini; Pavan, Paolo; Bertacchini, Alessandro; Larcher, Luca. - ELETTRONICO. - (2007), pp. 1-6. ( IWASI 2007 - 2nd International Workshop on Advances in Sensors and Interfaces Bari, Italy June 26-27, 2007) [10.1109/IWASI.2007.4420017].

IEEE

*Terms of use:*

The terms and conditions for the reuse of this version of the manuscript are specified in the publishing policy. For all terms of use and more information see the publisher's website.

18/12/2025 20:03

(Article begins on next page)

# Photovoltaic Cell Modeling for Solar Energy Powered Sensor Networks

D. Dondi\*, D. Brunelli\*\*, L. Benini\*\*, P. Pavan<sup>†</sup>, A. Bertacchini<sup>†</sup> and L. Larcher<sup>†</sup>

\*\*DEIS, Università di Bologna, Italy

\*DII, Università degli Studi di Modena e Reggio Emilia, Italy

<sup>†</sup>DISMI, Università degli Studi di Modena e Reggio Emilia, Italy

**Abstract**—Photovoltaic scavenging circuits have been presented to reduce installation and maintenance costs of wireless sensor networks. When small-size photovoltaic modules are adopted, optimizing the efficiency of the harvesting process and tracking the Maximum Power Point (MPP) becomes very difficult, and the development of a photovoltaic harvester has to be preceded by extensive simulations. The paper focuses on the definition of the model for a small PV cell allowing the simulation of harvester systems. The model is validated on a case study of MPPT circuit for sensor networks.

## I. INTRODUCTION

The vision of developing perpetual powered systems without a necessary periodical maintenance for battery replacement or recharging is one of the ultimate goals of sensor network design. In fact, although research continues to develop low power circuits, the amount of the energy provided by batteries or other storage devices still limits the operating lifetime of distributed embedded systems such as wireless sensor networks (WSN).

Photovoltaic (PV) harvesting circuits have been recently proposed to increase the autonomy of sensor nodes. An optimized circuit leads to several benefits such as: (i) minimization of the size of PV modules; (ii) adoption of smaller energy reservoirs; (iii) higher performance or better QoS by the supplied systems. The optimization of the energy collection under non stationary light conditions, is therefore certainly one of the major key design challenges. In particular when light irradiance is low, maximizing the efficiency of the harvesting process is critically important.

As the photovoltaic sources exhibit non-linear  $I$ - $V$  characteristics, which are dependent on irradiance and environmental factors, high-efficiency conversion systems usually adopt Maximum Power Point Tracking (MPPT) techniques to continuously deliver the highest possible power to the load. The problem, in fact, is to automatically find the voltage (and the current) at which the PV module has to operate in order to provide the maximum output power and to track its variations. These methods are generally exploited for large-scale PV power systems and are based on digital signal processor (DSP) or microcontrollers [1]. However with the increasing interest in harvesting technology for wireless sensor networks, MPPT techniques have been experimented also on small-scale PV power systems, tackling the development of circuits with power consumption of few mW. Under these

conditions the behavior of the PV integrated system has to be accurately modeled in order to optimize the scavenger at design-time.

Since the typical non-linear  $I$ - $V$  characteristic is represented with a complex analytical model without a closed-form solution [2], [3], development of an accurate circuit model is essential to simulate and implement a photovoltaic powered system [4]. In this paper a photovoltaic panel PSpice circuit-oriented model is presented, which accurately tracks the behavior of small PV cells over a wide range of irradiance conditions. We also describe a model characterization strategy that helps to rapidly extract model parameters from a small set of experiments. The model is then applied to a real design case study, namely a high-efficiency ultra low-power MPPT tracking circuit for environmentally powered wireless sensor networks.

The remainder of the paper is organized as follows. Related works are reviewed in the next section followed by the list of the contributions and the innovations that our work proposes. The theoretical model is discussed in section IV. Section V discusses the MPPT techniques adopted in our design case study and describes the actual implementation of a PV harvester. Experimental validation of the model in the case study design is reported in section VI, finally section VII concludes the paper.

## II. RELATED WORK

So far a complete design flow for solar harvesters which permits the simulation of user models, the synthesis and the verification of the final results, has been proposed only in large-scale PV systems (i.e. buildings), where the expertise in designing MPPT circuits is almost consolidated. In fact research in this field involves the study of the physics of PV arrays as well as the design of solar power conversion systems after intensive simulation steps [5], [6], [4].

Similar results are desirable also in scavenging circuits for wireless sensor networks. Better and more efficient converter systems may be developed by matching the harvesting circuit to the characteristics of the PV module. To the best of our knowledge nobody has yet supported the design of solar scavenger with complete and accurate simulations or developed a model for such circuits.

The first prototypes of energy scavengers were characterized directly by a connections between the PV panel and the energy

buffer (usually a supercapacitor), forcing the operating point to the capacitor voltage  $V_{CAP}$  [7], [8]. Moreover they do not perform any *MPP*, although the size of the panel permits to exploit some forms of power conversion management. Real *MPPT* system is instead *Everlast* [9], proposed by Chou et al. They exploit a microcontroller and analog circuits to track *MPP* during light variations. The size of the adopted *PV* modules is greater than  $20\text{cm}^2$  which is enough to provide tens of mW and to achieve an efficient power collection, but they did not perform any simulation to optimize the design of their circuit.

### III. CONTRIBUTIONS

The main contribution of this work is the introduction of a design flow for solar energy harvester which includes the characterization of the *PV* module and the simulation of the small-scale *PV* systems.

Compared to large-scale *PV* systems, small-size photovoltaic scavengers have to tackle the following issues: (a) the energy budget is small due to the size of the cells; (b) implementation of efficient *MPP* circuits usually takes large part of the power harnessed; (c) there is a substantial interaction between scavenger and the powered devices. This leads to the consideration that the design phase must be supported by simulations, in particular when conversion efficiency has to be optimized in cases of low insolation (e.g. in indoor applications). In order to fulfill this requirement, the paper presents the following contributions:

- We present a simple PSpice numerical model for small-size photovoltaic source, useful for integrated *PV* system design. The model is tailored to fit energy scavenger circuits for sensor nodes and it focuses on the emulation of the I-V relation over a wide range of irradiance intensity, cell temperature variation and incident angle.
- The validation of the model on a low-power photovoltaic harvesting circuit design example is also presented. The harvester tracks variations of the *MPP* and does not require any computational unit to find the suitable operating point of the *PV* module. As energy buffer the circuit works exploiting only supercapacitors, which have longer operating lifetime than batteries.

### IV. PHOTOVOLTAIC CELL MODELLING

The electrical power output delivered by a photovoltaic panel depends on the incident solar radiation, cell temperature, solar incidence angle and load resistance.

Manufacturers typically provide only few operational data for photovoltaic panels, such as the open circuit voltage ( $V_{oc}$ ), the short circuit current ( $I_{sc}$ ), the maximum power point voltage ( $V_{mpp}$ ) and current ( $I_{mpp}$ ), the temperature drift coefficients at open circuit voltage and short circuit current ( $\beta_{V_{oc}}$  and  $\alpha_{I_{sc}}$ , respectively). These data are usually available only at Standard Test Conditions (STC), for which the irradiance is  $1000\text{ W/m}^2$  and the panel temperature ( $T_C$ ) is  $25^\circ\text{C}$ . These conditions produce high power output, but are rarely

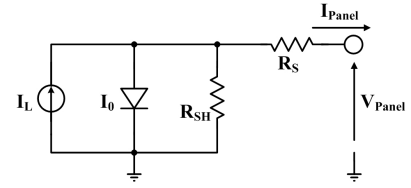


Fig. 1: Equivalent circuit of the *PV* cell representing the model parameters and the cell output.

encountered in actual operation environment and never reflect the indoor behavior.

Accurate, reliable and easy to apply methods for predicting the energy production of *PV* panels under variable working conditions are essential to allow optimum photovoltaic systems design and their customization related to the actual employment. For this reason the Photovoltaic Panel Model presented in this paper focuses on the prediction of *PV* output power over a wide range of environment condition.

The electrical power available from a panel can be modeled with the well known equivalent circuit shown in Fig. 1 [2]. The equivalent circuit contains a current generator that emulates the light generated current ( $I_L$ ), a diode to account for the typical knee of the current-voltage relation through the reverse saturation current ( $I_0$ ), a series resistor ( $R_S$ ) and a shunt resistor ( $R_{SH}$ ), emulating intrinsic losses depending on single *PV* cell series and parallel connections. In order to reproduce the electrical behavior of *PV* panel, this equivalent circuit requires some specific parameters that relate components values to the photovoltaic panel characteristics. These parameters could be extracted in two different ways: (i) exploiting an analytical extraction procedure, (ii) adopting a simplified procedure using some empirical relations. As described in following subsection, the analytical extraction procedure leads to a set of non-linear and implicit exponential equations, therefore a closed-form solution of the equations system is not available. While the *PV* panel description resulting by the presented simplified procedure provides a solution which depends only on panel implementation technology (i.e. mono- or polycrystalline silicon cells) and the particular working conditions.

#### A. Analytical parameter extraction procedure

The current-voltage relationship at a fixed cell temperature and solar insolation for the circuit in Fig. 1 is expressed in Eq. (1). Five parameters must be known in order to determine the current and voltage to evaluate the power delivered to the load. These parameters are: the light current ( $I_L$ ), the diode reverse saturation current ( $I_0$ ), the series resistance ( $R_S$ ), the shunt resistance ( $R_{SH}$ ), and the modified panel ideal factor ( $a$ ) defined in Eq. (2).

$$I_{\text{panel}} = I_L - I_0 \left( e^{\frac{V_{\text{panel}} + I_{\text{panel}} R_S}{a}} - 1 \right) - \frac{V_{\text{panel}} + I_{\text{panel}} R_S}{R_{SH}} \quad (1)$$

$$a \equiv \frac{N_S \eta k T_C}{q} \quad (2)$$

The electron charge  $q$  and the Boltzmann's constant  $k$  are known values;  $\eta$  is the usual photovoltaic single cell ideal factor (which value varies within  $1 \div 2$ ),  $N_S$  is the number of cells in series and  $T_C$  is the *PV* panel temperature [2].

The power delivered by the *PV* panel correspond to the product of the output current ( $I_{\text{panel}}$ ) and voltage ( $V_{\text{panel}}$ ) at a particular working condition.

The five parameter appearing in Eq. (1) corresponding to operation at STC are designated:  $a_{ref}$ ,  $I_{L,ref}$ ,  $I_{0,ref}$ ,  $R_{S,ref}$  and  $R_{SH,ref}$ . In general, these five parameters are functions of the solar radiation incident on the panel and the panel temperature. Reference values of these parameters are determined for a specified working condition, such as STC.

To evaluate these five parameters in Eq. (1), a system of five independent equations is needed. Three current-voltage relations are normally available from the manufacturer at STC: the short circuit current, the open circuit voltage and the current and voltage at the maximum power point, Eqns. (3) - (5). Fourth equation results from recognizing that the derivative of the power at the maximum power point should be zero, Eqn. (6).

For short circuit current:  $I_{\text{panel}} = I_{sc,ref}$ ,  $V_{\text{panel}} = 0$

$$I_{sc,ref} = I_{L,ref} - I_{0,ref} \left( e^{\frac{I_{sc,ref} R_{S,ref}}{a_{ref}}} - 1 \right) - \frac{I_{sc,ref} R_{S,ref}}{R_{SH,ref}} \quad (3)$$

For open circuit voltage:  $I_{\text{panel}} = 0$ ,  $V_{\text{panel}} = V_{oc,ref}$

$$0 = I_{L,ref} - I_{0,ref} \left( e^{\frac{V_{oc,ref}}{a_{ref}}} - 1 \right) - \frac{V_{oc,ref}}{R_{SH,ref}} \quad (4)$$

At the maximum power point:  $I_{\text{panel}} = I_{mpp,ref}$ ,  $V_{\text{panel}} = V_{mpp,ref}$

$$I_{mpp,ref} = I_{L,ref} - I_{0,ref} \left( e^{\frac{V_{mpp,ref} + I_{mpp,ref} R_{S,ref}}{a_{ref}}} - 1 \right) - \frac{V_{mpp,ref} + I_{mpp,ref} R_{S,ref}}{R_{SH,ref}} \quad (5)$$

The derivative of output power with respect to panel output voltage at the maximum power point is zero.

$$\left. \frac{d(VI)}{dV} \right|_{mpp} = I_{mpp} + V_{mpp} \left. \frac{dI}{dV} \right|_{mpp} = 0 \quad (6)$$

This approach provides only a system of four non-linear and implicit exponential equations. To obtain the desired model parameters for the evaluation of the output current and voltage, the equations system should be solved as function of one of them. Therefore an iterative approach is needed, such as with the Levenberg-Marquardt method [3].

For this reason the analytical model has been dropped and parameter have been extracted using the procedure described in following subsection.

### B. Simplified parameters extraction procedure

Since different *PV* panel implementation technologies imply very different current-voltage relation profiles, an accurate PSpice model parameters extraction is needed to describe the panel behavior. In particular: mono-crystalline silicon cells exhibit an initial flat current-voltage slope with a sharp knee, while poly-crystalline and amorphous silicon cells exhibit a current-voltage slope with a smooth knee spanning over a large voltage range. The parameter extraction procedure proposed in this paper allows to obtain a complete description of *PV* panel electrical characteristics over an extended range of insolation conditions and concerning all kind of implementation technologies.

This is possible dimensioning components involved in *PV* panel equivalent circuit shown in Fig. 1 with some accurate observations of *PV* panel output. Implementation technology dependent fixed parameters, such as  $R_S$  and  $R_{SH}$ , can be determined through an approximated measured current-voltage relation curve fitting. To fit a real *PV* panel characteristic once fixed parameters have been determined, insolation and temperature dependent parameters can be determined using simplified relations derived from Eqn. (4).

In fact, in first approximation, it is possible to assume that the short circuit current ( $I_{sc}$ ) is equal to the generated light current ( $I_L$ ) [6], consequently the equation that relates the short circuit current and open circuit voltage becomes:

$$I_{sc} = I_0 \left( e^{\frac{q V_{oc}}{k T_C}} - 1 \right) + \frac{V_{oc}}{R_{SH}} \quad (7)$$

Assuming that the ratio between  $V_{oc}$  and  $R_{SH}$  is negligible because of  $R_{SH}$  is typically several *kilo-ohms*, the diode saturation current determines the open-circuit voltage ( $V_{oc}$ ) of the *PV* panel, and can be extracted from (7) as shown in (8)

$$V_{oc} = \left( \frac{k T_C}{q} \right) \ln \left( \frac{I_{sc}}{I_0} + 1 \right) \quad (8)$$

Furthermore, extraction of insolation and temperature model parameter dependency involves a couple of well known physical relations [2] [6]; Eqn. (9) provides  $I_0$  and Eqn. (10) provides  $I_L$ .

$$I_0 = I_{0,STC} \left( \frac{T_C}{T_{ref}} \right)^3 e^{\left( \frac{q E_G}{k T_C} \right) \frac{1}{T_{ref}} - \frac{1}{T_C}} \quad (9)$$

$$I_L = I_{L,STC} S + \alpha_{I_{sc}} \left( \frac{1}{T_{ref}} - \frac{1}{T_C} \right) \quad (10)$$

$S$  is the solar insolation expressed in  $[W/m^2]$  and  $T_C$  is the *PV* panel working temperature in  $[K]$ .  $I_{0,STC}$  is extracted from Eqn. (7) imposing STC working condition, while  $I_{L,STC}$  is determined considering that, at zero output voltage,  $I_L$  is equal to the short-circuit current  $I_{sc}$ . Using these relations the model has been verified and compared with the measurement results validating the model performances. Panel current and power characterization reported in Fig. 2 and Fig. 3, have been carried out with a customized set-up based on a halogen light source. The employment of a halogen light source implies a gradual

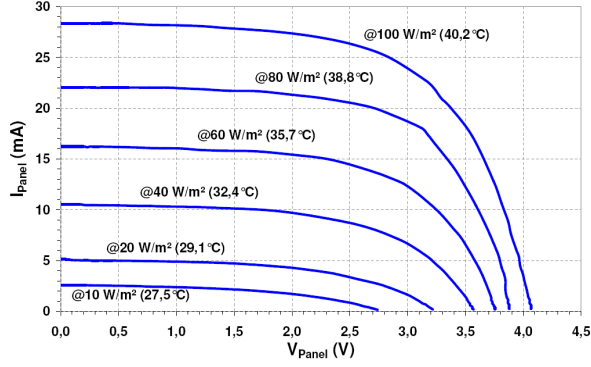


Fig. 2: Photovoltaic cell output current measured at different indoor insolation condition with data correction to scale current values at the equivalent temperature of  $25^{\circ}\text{C}$ .

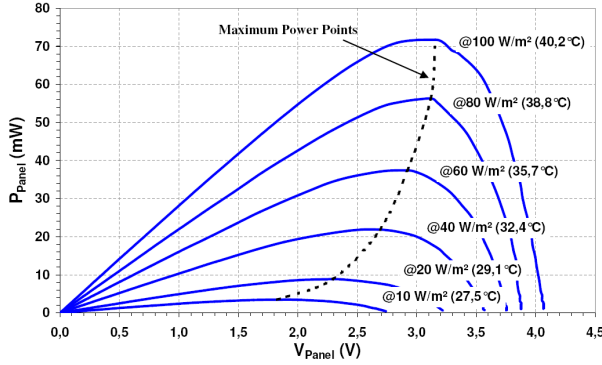


Fig. 3: Photovoltaic cell output power measured at different indoor insolation condition with data correction to scale power values at the equivalent temperature of  $25^{\circ}\text{C}$ .

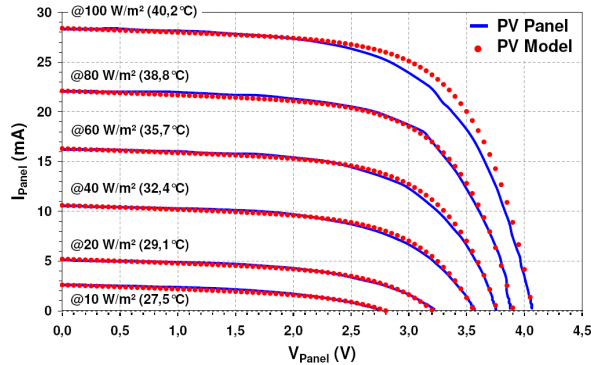


Fig. 4: Comparison of *PV* panel PSpice model output current with measured output current at indoor illumination, from  $10\text{ W/m}^2$  to  $100\text{ W/m}^2$ .

panel overheating increasing the light intensity. The main drawback of this set-up is that many panels suffer a thermal drift phenomena. In order to obtain a reliable characterization, thermal drift correction has been applied to measured data. The correction exploits thermal drift coefficients,  $\beta_{V_{OC}}$  and  $\alpha_{I_{SC}}$ , to scale all curves to the one provided at the equivalent temperature of  $25^{\circ}\text{C}$ . In this way the characterization is

exclusively affected by light intensity variation performed at an equivalent constant temperature.

Fig. 4 shows the comparison of real panel measurements with proposed model simulations at different indoor insolation conditions. Results analysis validates the proposed model parameters extraction procedure.

## V. SOLAR ENERGY HARVESTER CASE STUDY

### A. MPPT techniques

There are several methods and algorithms to analyze and find the *MPP*, certainly the most used are *Perturb and Observe (P&O)* [10] and *Fractional Open-Circuit Voltage (FOC)* [11]. *P&O* method is widely used for large *PV* systems, because it is very accurate but exploits DSPs or microcontrollers, which consume non-negligible power. Fractional Open-Circuit Voltage (*FOCV*) is the most used and cost-effective in small-scale *PV* systems. This method exploits the nearly linear relationship between the operating voltage at *MPP* ( $V_{MPP}$ ) of a *PV* module and the open circuit voltage ( $V_{OC}$ ).

$$V_{MPP} \approx K_{FOC} \cdot V_{OC} \quad (11)$$

where the proportional constant  $K_{FOC}$  belongs to the interval (0.71, 0.78). Table I shows the behavior of the constant ( $K_{FOC}$ ) of the solar cell used, under different irradiance conditions.

$S [\text{W/m}^2]$	$V_{mpp} [\text{V}]$	$V_{oc} [\text{V}]$	$K_{FOC}$
20	2.29	3.23	0.71
40	2.69	3.58	0.75
60	2.92	3.76	0.78
80	3.08	3.98	0.77
100	3.12	4.01	0.78
200	3.17	4.10	0.78
400	3.19	4.16	0.77
600	3.24	4.21	0.76
800	3.27	4.26	0.77
1000 (STC)	3.29	4.29	0.78

TABLE I: Fractional Open-Circuit Voltage, relation between  $V_{oc}$  and  $V_{mpp}$  at different light conditions.

The *MPP* can be approximated measuring periodically  $V_{oc}$  by a temporary disconnection of the *PV* module from the circuit. Of course this is a disadvantage because of the transient drop of power. To overcome this problem, we exploit an additional small *PV* module acting as pilot cell, which matches the characteristics of the principal *PV* array. We adopt the CPC1824 from Clare, Inc [12]. It is a monolithic photovoltaic string of solar cells of only  $0.1\text{ cm}^2$ , and it is used as light insolation sensor to provide feedback information for the tracker.

Since the pilot cell has been manufactured with the same technology of the *PV* panel, it has been assumed that the output current of the pilot cell follows linearly the behavior of the solar panel during light variations. In a custom implementation of the harvesting circuit, this assumption leads to consider the pilot cell as a single cells of the whole main *PV* array.

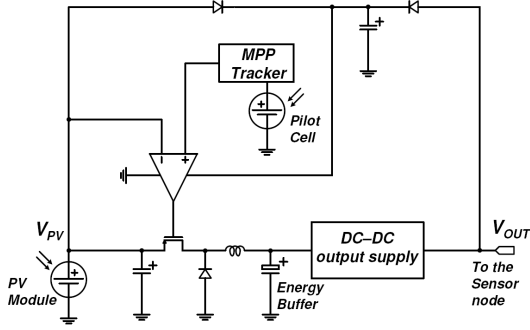


Fig. 5: Schematic diagram of the harvester platform

Following these assumptions, several simulations have been carried out to validate the maximum power point tracker at different light conditions. Table II shows the comparison between the simulated maximum power point voltage imposed by the MPP tracker ( $V_{mpp, sim}$ ) with the optimum maximum power point voltage measured during the *PV* panel characterization ( $V_{mpp, meas}$ ). MPP tracker validation confirms that the adopted approach lead to a *PV* panel polarization within a 5% from the ideal working conditions.

$S [W/m^2]$	$V_{mpp, sim} [V]$	$V_{mpp, meas} [V]$	Error [%]
10	1.91	1.83	+ 4,4
20	2,38	2,29	+ 4,0
40	2,67	2,69	- 0,7
60	2,82	2,92	- 3,4
80	2,94	3,08	- 4,5
100	3,00	3,12	- 3,9
200	3,01	3,17	- 4,6
400	3,14	3,19	- 1,6
600	3,15	3,24	- 2,9
800	3,16	3,27	- 3,2
1000 (STC)	3,18	3,29	- 3,3

TABLE II: Validating the MPP Tracker over a wide range of illumination conditions through comparison of simulated mpp voltage ( $V_{mpp, sim}$ ) with the measured *PV* panel ideal mpp voltage ( $V_{mpp, meas}$ ).

### B. Solar scavenger architecture

The hardware architecture of the solar scavenger adopted as a case study, is displayed in Fig. 5 and it has been designed after several simulation steps using the proposed model for *PV* array. We adopt a buck configuration as power converter between *PV* module and the storage device, since the solar cell's nominal voltage is higher than the values reachable by the energy buffer. As pointed out in sec. V-A, the *Fractional Open-Circuit* method is exploited by matching  $V_{panel}$  to the estimated  $V_{mpp}$  using a pilot-cell as input signal. The ultra-low power comparator adopted bounds the buck converter to work inside a voltage range around *MPP*. Narrowing the windows around estimated *MPP* means to operate at higher switching frequencies, with higher conversion efficiency, on the other hand it requires a faster comparator, which is generally more power consuming. Finally an integrated step-up converter is

adopted to provide a fixed voltage supply to the wireless sensor node. The whole scavenger is powered by the main *PV* module when the final DC/DC is shut down because the voltage of the energy buffer is not enough to start it up. This permits to reduce the power consumption during the initial phase of the energy buffer charging procedure and then increase the overall performance.

## VI. EXPERIMENTAL RESULTS

The solar scavenger, proposed as case study, has been extensively characterized in order to compare and validate the simulation results. The performance of the implemented circuit has been investigated by measuring the charging efficiency of the energy buffer and measuring the power consumed by the *MPPT* system.

### A. Scavenging efficiency

We consider the following equations which define the efficiency of a power conversion:

$$\eta = \frac{P_{transferred}}{P_{MPP}} \quad (12)$$

$$P_{MPP} = V_{MPP} \cdot I_{MPP} \quad (13)$$

$$P_{transferred} = \frac{1}{2} \frac{C}{T} [V^2(t) - V^2(t - T)] \quad (14)$$

Where  $P_{MPP}$  is the power at the *MPP*,  $P_{transferred}$  is the average power transferred in the energy buffer. When supercapacitors are adopted, it is usually computed as the value necessary to increase the energy level from  $E(t_1 - T)$  to  $E(t_1)$  during a given time interval  $T$ . In our tests,  $\eta$  has been evaluated considering also the DC/DC converter which affects the result with its own intrinsic losses. Fig. 6 shows the efficiency of the method proposed during the refilling of the energy buffer over elapsed time. The curve with triangles represents the linear charging behavior with a direct connection between the *PV* panel and the storage device. The curve with squares, instead shows the trend when the harvester circuit is powered only using the final DC/DC converter. In this case the harvester works properly only after the DC/DC starts up as evidenced by a change in the slope. The charging behavior using the proposed energy scavenger is plotted with the curve with dots. The curve approaches well the simulation result obtained using the model of our *PV* cells (continuous curve). Fig. 7 shows the efficiency, defined as in (12), over the time. Looking at the curve with squares, it is more evident that only when the level of the energy buffer is sufficient to turn the DC/DC on, the scavenger can work properly and increase the efficiency. Finally the curve with dots approaches the simulations results with an error less than 5% and represents the efficiency when the scavenger is powered also by the *PV* cell. It is important to remark that the model covers irradiance variations as well as temperature changes of the *PV* array. Under light irradiance, heat affects the performance of the scavenger smoothing the efficiency increment, and simulations take in account this effect. Using the model with the assumption of constant temperature, simulation results

diverge from the actual efficiency by more than 10%, as shown in Fig. 8.

### B. Power consumption

Adopting the proposed model for the design of the solar harvester, we have also built a *MPPT* circuit with very low power consumption. In fact, when the switch in the buck power converter is open, the overall power consumption of the circuit is less than half a *mW*. ( $P_{switch-off} \approx 300\mu W$ ). Values of

about  $1mW$  ( $P_{switch-on}$ ) happen as soon as the comparator switches the MOS transistor on to replenish the energy buffer. Therefore the average power can be easily computed using the following equation.

$$P = D \cdot P_{switch-off} + (1 - D) \cdot P_{switch-on} \quad (15)$$

Since the duty cycle of the switch is typically higher than 80% also in indoor conditions, the average power consumed by both the buck and the control circuit is below  $1mW$ .

## VII. CONCLUSION

In this paper we have presented a *PV* cell model for solar energy powered sensor networks, suitable over a wide range of irradiance intensity, cell temperature variation and incident angle. An implementation of a solar scavenger optimized for indoor environments, using the model and simulations, has been also presented as case study. Finally, experimental results have validated the proposed model for small-size *PV* arrays.

## REFERENCES

- [1] C. Hua and C. Shen, "Study of maximum power tracking techniques and control of dc/dc converters for photovoltaic power system," in *Power Electronics Specialists Conference, 1998. PESC 98 Record. 29th Annual IEEE*, vol. 1, pp. 86–93vol.1, 17–22 May 1998.
- [2] W. De Soto, S. Klein, and W. A. Beckman, "Improvement and validation of a model for photovoltaic array performance," *Solar Energy*, vol. 80, pp. 78–88, Jan 2006.
- [3] J. Gow and C. Manning, "Development of a photovoltaic array model for use in power-electronics simulation studies," in *Electric Power Applications, IEE Proceedings*, vol. 146, pp. 193 – 200, 1999.
- [4] S. Foss, B. Olaisen, E. Marstein, and A. Holt, "A new 2.5d distributed spice model of solar cells," in *European Photovoltaic Solar Energy Conference and Exhibition*, no. 21, (Dresden), 2006.
- [5] G. Yu, Y. Jung, J. Choi, I. Choy, J. Song, and G. Kim, "A novel two-mode mppt control algorithm based on comparative study of existing algorithms," in *Photovoltaic Specialists Conference, 2002. Conference Record of the Twenty-Ninth IEEE*, no. 19–24, pp. 1531 – 1534, May 2002.
- [6] K. Phani Kiranmai and M. Veerachary, "Maximum power point tracking: A pspace circuit simulator approach," in *Power Electronics and Drives Systems, 2005. PEDS 2005. International Conference on*, vol. 2, pp. 1072 – 1077, Nov 2005.
- [7] X. Jiang, J. Polastre, and D. E. Culler, "Perpetual environmentally powered sensor networks,," in *Proceedings of the Fourth International Symposium on Information Processing in Sensor Networks, IPSN 2005*, (UCLA, Los Angeles, California, USA), pp. 463–468, April 25–27 2005.
- [8] V. Raghunathan, A. Kansal, J. Hsu, J. Friedman, and M. B. Srivastava, "Design considerations for solar energy harvesting wireless embedded systems,," in *Proceedings of the Fourth International Symposium on Information Processing in Sensor Networks, IPSN 2005*, (UCLA, Los Angeles, California, USA), pp. 457–462, April 25–27 2005.
- [9] F. Simjee and P. H. Chou, "Everlast: long-life, supercapacitor-operated wireless sensor node,," in *ISLPED '06: Proceedings of the 2006 international symposium on Low power electronics and design*, (New York, NY, USA), pp. 197–202, ACM Press, 2006.
- [10] Y.-C. Kuo, T.-J. Liang, and J.-F. Chen, "Novel maximum-power-point-tracking controller for photovoltaic energy conversion system," *Industrial Electronics, IEEE Transactions on*, vol. 48, pp. 594–601, June 2001.
- [11] D.-Y. Lee, H.-J. Noh, D.-S. Hyun, and I. Choy, "An improved mppt converter using current compensation method for small scaled pv-applications," in *Applied Power Electronics Conference and Exposition, 2003. APEC '03. Eighteenth Annual IEEE*, vol. 1, pp. 540–545vol.1, 9–13 Feb. 2003.
- [12] Clare, Inc., "Clare solar cells - cpc series data sheet," (<http://www.clare.com/Products/SolarCell.htm>), August, 2005.

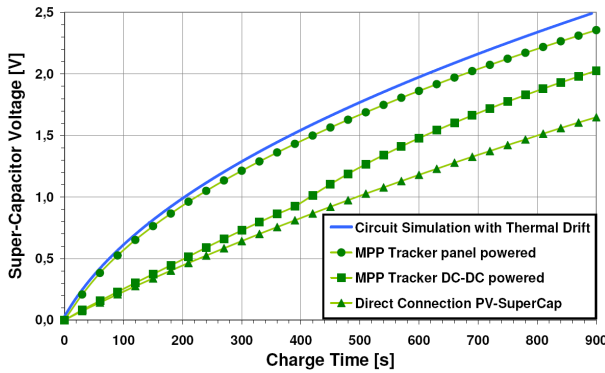


Fig. 6: Comparison of the supercapacitor charge simulation curve with performance of three different implementations of the harvesting circuit

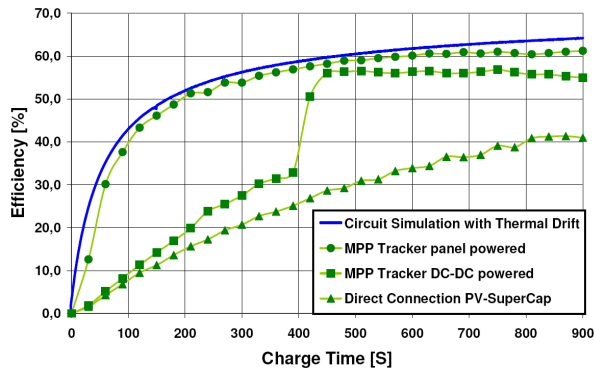


Fig. 7: Comparison of the efficiency between simulation and three different implementations of the harvesting circuit.

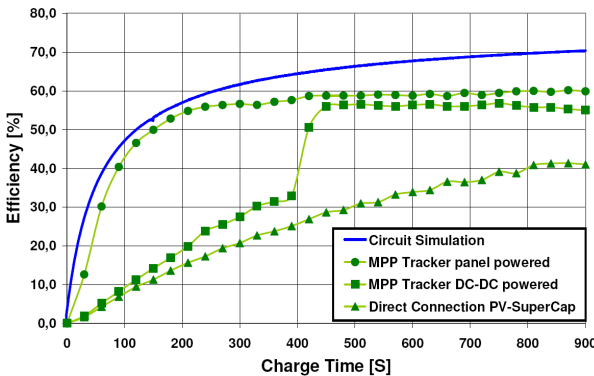


Fig. 8: Comparison of the efficiency between same circuit measurements and simulation results without overheating.